WATER RESOURCES RESEARCH, VOL. 35, NO. 1, PAGES 17–27, JANUARY 1999

Laboratory investigations of effective flow behavior in unsaturated heterogeneous sands

D. Wildenschild[1] and K. H. Jensen

Department of Hydrodynamics and Water Resources, Technical University of Denmark, Lyngby

Abstract. Two-dimensional unsaturated flow and transport through heterogeneous sand was investigated under controlled laboratory conditions. The unsaturated hydraulic conductivity of five homogeneous sands and three heterogeneous systems composed of these five sands was measured using a steady state flux controlled method. The heterogeneous sand systems were established in a laboratory tank for three realizations of random distributions of the homogeneous sands comprising a system of 207 grid cells. The water flux was controlled at the upper boundary, while a suction was applied at the lower boundary such that on the average a uniform pressure profile was established and gravity flow applied. Solute breakthrough curves measured at discrete points in the tank using time domain reflectometry, as well as dye tracer paths, showed that flow and transport took place in a very tortuous pattern where several grid cells were completely bypassed. The degree of tortuosity appeared to be dependent on the degree of saturation, as the tortuosity increased with decreasing saturation. Despite the tortuous flow patterns, we found that the effective unsaturated hydraulic conductivity as well as the retention curves for the three realizations of the heterogeneous sand were quite similar, thus suggesting that this type of heterogeneous flow system can be treated as an equivalent homogeneous medium characterized by effective parameters.

1. Introduction

Field soils are inherently heterogeneous. Research in the past couple of decades has shown that spatial variability in hydraulic properties has a considerable influence on flow and transport through porous media. Several theoretical [*Zaslavsky and Sinai*, 1981a, b; *Mualem*, 1984; *Yeh et al*., 1985a, b, c; *Mantoglou and Gelhar*, 1987a, b, c; *Mantoglou*, 1992] and experimental studies, both in the laboratory [e.g., *Stauffer and Dracos*, 1986; *Stephens and Heermann*, 1988; *Yeh and Harvey*, 1990; *Sassner et al*., 1994; *Destouni et al*., 1994] as well as in the field [e.g., *Nielsen et al*., 1973; *Wierenga et al*., 1986; *Butters et al*., 1989; *Hills et al*., 1991; *Jensen and Refsgaard*, 1991a, b, c; *McCord et al*., 1991a; *Jensen and Mantoglou*, 1992] have demonstrated the significance of heterogeneity on both flow and transport in unsaturated soils. For example, extensive field experiments were carried out at the Las Cruces trench site [*Wierenga et al*., 1986, 1991], to investigate the effects of spatial variability on water flow and contaminant transport in unsaturated soils. As expected, a high level of spatial variability in saturated hydraulic conductivity was reported for the site (a standard deviation of 647 cm/d around a mean of 533 cm/d). In subsequent modeling efforts, *Wierenga et al*. [1991] found that simple deterministic models were able to adequately predict the overall movement of the wetting front through the soil during infiltration but that they gave poor predictions of point values of the water content due the spatial variability of the soil. Modeling efforts on the Las Cruces field experiments were also reported by other researchers. For instance, *Polmann et al*. [1988, 1991] investigated the applicability of stochastic methods (using *Mantoglou and Gelhar*'s [1987a, b, c] theory) for simulating large-scale unsaturated flow and transport observed at the site. They confirmed the hypothesis of *Mantoglou and Gelhar* [1987b, c] that large-scale effective hydraulic properties exhibit hysteresis and anisotropy. Similar investigations were carried out by *Jensen and Refsgaard* [1991a, b, c] and *Jensen and Mantoglou* [1992], with the latter study concluding that simulations based on a stochastic representation of spatial variability provided better predictions of both the capillary tension and the water content than a more traditional deterministic description.

Regardless of whether the soil behaves as an isotropic or anisotropic medium or is subject to hysteresis the spatial variability of soil hydraulic properties and their variation with saturation have to be considered in order to provide realistic predictions of unsaturated flow and transport at the field scale. Given the significant and often erratic variability of hydraulic parameters in the field, it is impractical to deterministically characterize the variability in complete detail. Furthermore, the computational demand by a numerical model would be enormous if the variability at all scales is to be considered. An alternative approach, used by several of the above mentioned investigators, is to treat the soil as an equivalent homogeneous medium characterized by effective parameters so that the average flow behavior can be predicted. This approach transfers the heterogeneity problem to the identification of effective parameters.

One possible, and elaborate, method for obtaining effective parameters is to conduct large-scale field experiments and use inverse techniques for parameter estimation. Another approach is to derive the effective parameters from simple statistical averages of the local properties or, alternatively, relate

[1]Now at Department of Earth and Environmental Sciences, Lawrence Livermore National Laboratory, Livermore, California.

Paper number 98WR01958.
0043-1397/99/98WR-01958$09.00

the effective parameters to the variability of the small-scale soil parameters using stochastic theories in which the hydraulic parameters are considered random functions. To fully assess the usefulness of the various approaches field-scale experimentation is required. A few studies that compare predictions of the stochastic theories of *Yeh et al*. [1985a, b, c] and *Mantoglou and Gelhar* [1987a, b, c] to field measurements [e.g., *McCord et al*., 1991a, b; *Jensen and Mantoglou*, 1992] have been carried out over the last decade. Unfortunately, field experiments are difficult to carry out and always involve some uncertainty associated with the correct implementation of boundary conditions, or the representativeness of spatial soil sampling schemes (local hydraulic properties), among other factors. A step toward validation of the concept of effective parameters is to carry out controlled laboratory experiments, where boundary conditions and the true distribution of soil types are known.

Yeh and Harvey [1990] tested the effective hydraulic conductivity concept in one dimension by performing vertical infiltration experiments on layered soil columns in the laboratory and, subsequently, comparing measured hydraulic conductivities to estimates obtained by simple statistical averages and by a stochastic approach. A one-dimensional experiment restricts water flow by not allowing water to follow pathways of least resistance. Tests that more closely represent a field condition require the use of more than one dimension. The aim of the present study was to carry out detailed two-dimensional laboratory experiments, where the soil configuration was controlled and the hydraulic properties were measured in detail. Investigating flow in two dimensions may still be a limitation relative to having a complete three-dimensional experimental description of the unsaturated flow process. However, the errors introduced by going from three-dimensional to far less cumbersome two-dimensional experiments should be considerably less detrimental to studies of soil heterogeneity than errors introduced by forcing flow and transport to be restricted to only one dimension. Thus the main objectives of the present study are to (1) study flow processes in a two-dimensional heterogeneous system and (2) establish quantitative data sets for testing numerical models and theories, particularly the concept of effective parameters. In a subsequent paper [*Wildenschild and Jensen*, this issue] the measured effective parameters are compared with parameters based on different statistical representations of spatial variability, including a stochastic approach. These statistical parameter estimates are subsequently incorporated in a numerical model and tested against transient laboratory data.

2. Experimental Procedures

2.1. Flow

The study consisted of a series of infiltration experiments conducted in a laboratory tank of dimensions of $100 \times 110 \times 8$ cm^3 and packed with sand in known heterogeneous configurations (Figure 1). The tank was constructed of clear acrylic plastic and sealed with rubber o-rings and lining. Prior to use, one side of the tank was cut horizontally at the center so that the top part could be removed to enable packing. A box with a built-in porous plate was machined to fit accurately in the bottom of the tank and used to control flow under suction. The box consisted of a 3 cm high acrylic plastic water reservoir with a 4 mm thick sintered bronze plate (air-entry pressure of $\sim$140 cm) machined to fit on top, and thus the porous plate covered the entire horizontal extent of the tank. The clear acrylic plastic facilitated easy detection of entrapped air. The porous plate was boiled in distilled water prior to its use to remove entrapped air and attached to the acrylic plastic reservoir while submerged in water. Once assembled, the suction box was lowered into the tank. The suction box contained two brass ports and 8 mm ID rigid tubing to enable flushing of the reservoir when in use and to provide an outlet for water during the experiments. We experienced several problems with this prototype plate design, particularly with air leaks along the lining and because the relatively low air-entry pressure of the plate was quite easily exceeded. In both cases, the entire tank had to be emptied and repacked with sand after the problem was solved.

Five different, commercially available, homogeneous sands were used in the experiments (the hydraulic characteristics of the five sands are discussed later in this section). A statistically uniform distribution of the different sands in the experimental tank was assured by using a random number generator to assign soil types to a predesigned two-dimensional grid. The sizes of the individual heterogeneities in the two-dimensional grid were cells of $5 \times 10 \times 8$ cm^3 (height $\times$ length $\times$ width) and $5 \times 5 \times 8$ cm^3 (Figure 1). The particular system of heterogeneities was purposely chosen to accommodate a distinctly heterogeneous two-dimensional flow field. Hence flow was not restricted by extended hydraulic barriers in the tank, such as would be the case in a layered system. Furthermore, the system was designed to conform at least partially to the assumptions of stochastic theory. Among these assumptions was the demand that the scale of heterogeneity (correlation length) was much smaller than the overall scale of the problem, which implied that the size of the heterogeneities (the grid cells) should be 1/10 or less of the extent of the flow flume [*Yeh et al*., 1985a]. Considering these requirements the heterogeneities were chosen to be 10 cm long and 5 cm high. The smaller ($5 \times 5 \times 8$ cm^3) size cells were needed at the end of every other layer (Figure 1) to allow a shift in the cell boundaries horizontally, so that they were not located directly above each other. Ideally, even smaller heterogeneities should have been used to strictly conform to the stochastic theory of *Mantoglou and Gelhar* [1987a, b, c]; a packing with such small cell units was judged to be infeasible.

The tank was packed according to a given random distribution, with the first realization illustrated in Figure 1 and a second realization in Figure 2. A set of spatulas of adjustable width was used for separating the individual grid cells during packing. Sand within each cell was compacted to approximate the packing used when measuring the hydraulic properties of the individual homogeneous sands (see the discussion of porosities in section 3.1). Tensiometers and time domain reflectometry (TDR) probes were installed during packing, and the water level was raised several times to the level of packing to avoid extremely high suctions on the tensiometer cups.

An array of 30 tensiometers and 12 TDR probes were placed in a two-dimensional pattern on one side of the tank (Figure 1) to measure capillary suction and water content, respectively. The locations of the different tensiometers and TDR probes are further shown in Figure 2. Tensiometers and TDR probes were held in place by rubber stoppers. The tensiometers were made of ½ bar, 0.65 cm diameter porous ceramic cups obtained from Königliche Porzellän Manufaktur Berlin, GmbH, Germany, and cut to a length of 3 cm. Transducers with amplifiers were attached to the outlet end of the tensiometers and connected to a computer for automatic monitoring. The TDR

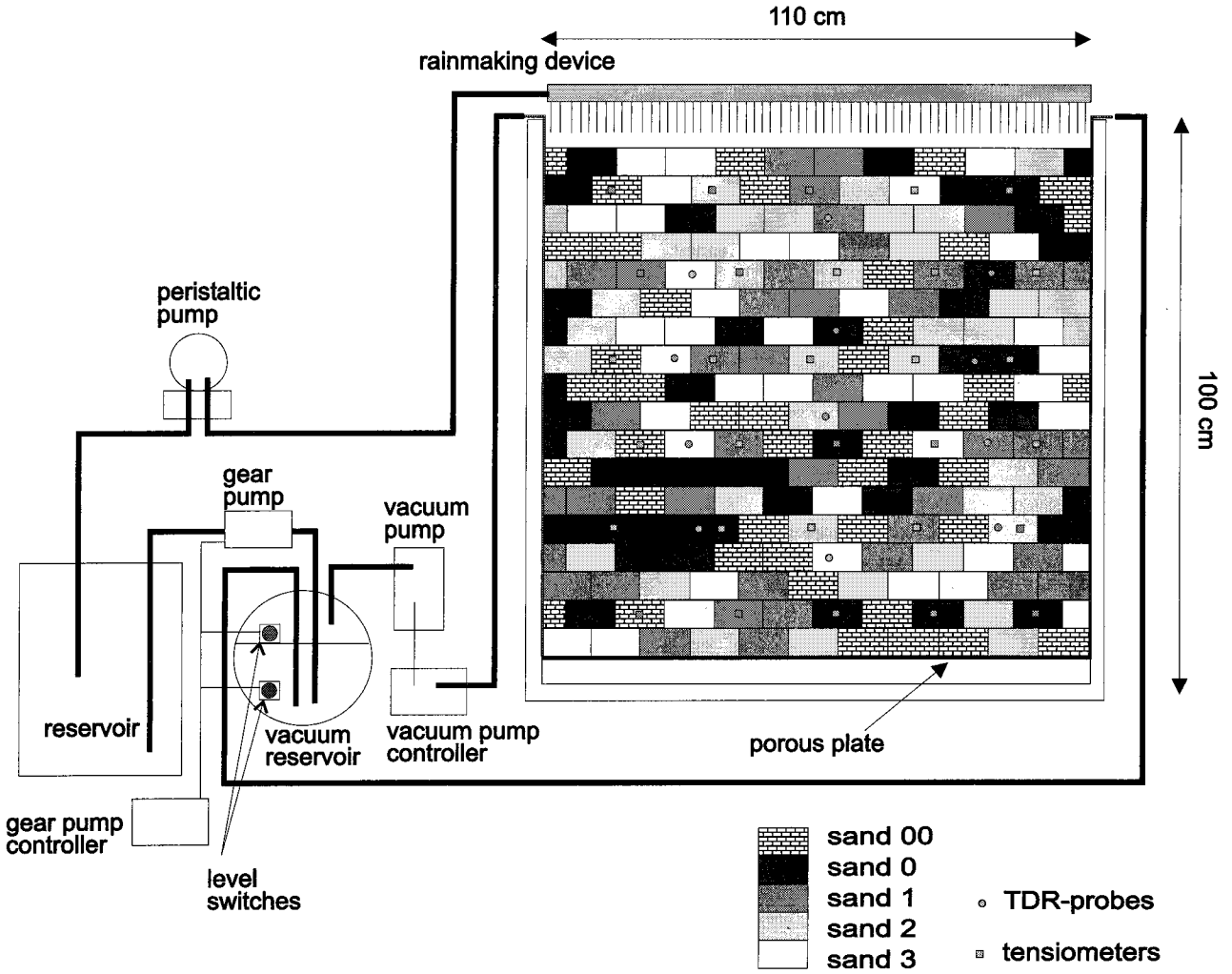

Figure 1. Laboratory setup for the two-dimensional tank experiment.

probes (waveguides) were constructed of pairs of parallel stainless steel rods, 0.5 cm apart with a diameter of 0.16 cm and 7 cm long, placed in an acrylic casing. A Tektronix cable tester (model 1502B), connected to a computer-controlled multiplexer, was used for scanning the 12 TDR probes. The TDR-probes were calibrated against gravimetric water contents in separate experiments, and a curve was established for each individual probe. Three-parameter empirical relationships were used for the calibration, rather than the commonly used expression of *Topp et al*. [1980]. The water flux out of the tank was measured automatically by a pulse flow meter, except at very low flow rates when measurements were made manually.

Water was supplied to the top of the tank by means of a peristaltic pump and distributed evenly over the entire boundary by a rainmaking device consisting of an acrylic plastic reservoir covering the entire surface of the tank with an array of 115 hypodermic needles distributing the water (23 needles in 5 offset rows). The suction at the lower boundary of the tank was controlled by a system of transducers and vacuum and gear pumps (Figure 1). The vacuum pump was used to supply the necessary suction for establishing a uniform average pressure profile in the tank. This pump was controlled by a transducer that would switch the pump off and on as the required suction demand in the reservoir underneath the porous plate was met or not. A gear pump used for emptying the vacuum reservoir was controlled by a set of two level switches placed in the reservoir. The level switches would turn the gear pump on and off in response to the fluctuating water level in the reservoir. When the gear pump was activated to lower the excess pressure in the reservoir, a magnetic valve (bleeder) was opened automatically with the onset of the gear pump and closed again when the pump stopped. The actual physical connection from the devices providing the suction to the water reservoir under the porous plate was established through a line of rigid Teflon tubing going from the bottom of the tank, up through the sand in one corner of the tank, and back down to the vacuum pump. Ideally, the applied suction should be the same as the steady state suction profile we tried to establish in the tank, thus implying an iterative procedure. However, clogging of the porous plate in certain cases forced us to use higher suctions underneath the plate to guarantee sufficient suction in the soil above the plate. We found later that the magnitude of the applied suction was not critical to the creation of a steady state flow regime in the tank. The applied flow rate was the controlling factor; as long as the imposed bottom suction was higher than the level we were trying to establish for the tank as a whole, it did not negatively influence the flow conditions in the tank. Even when the imposed suction at the plate was much

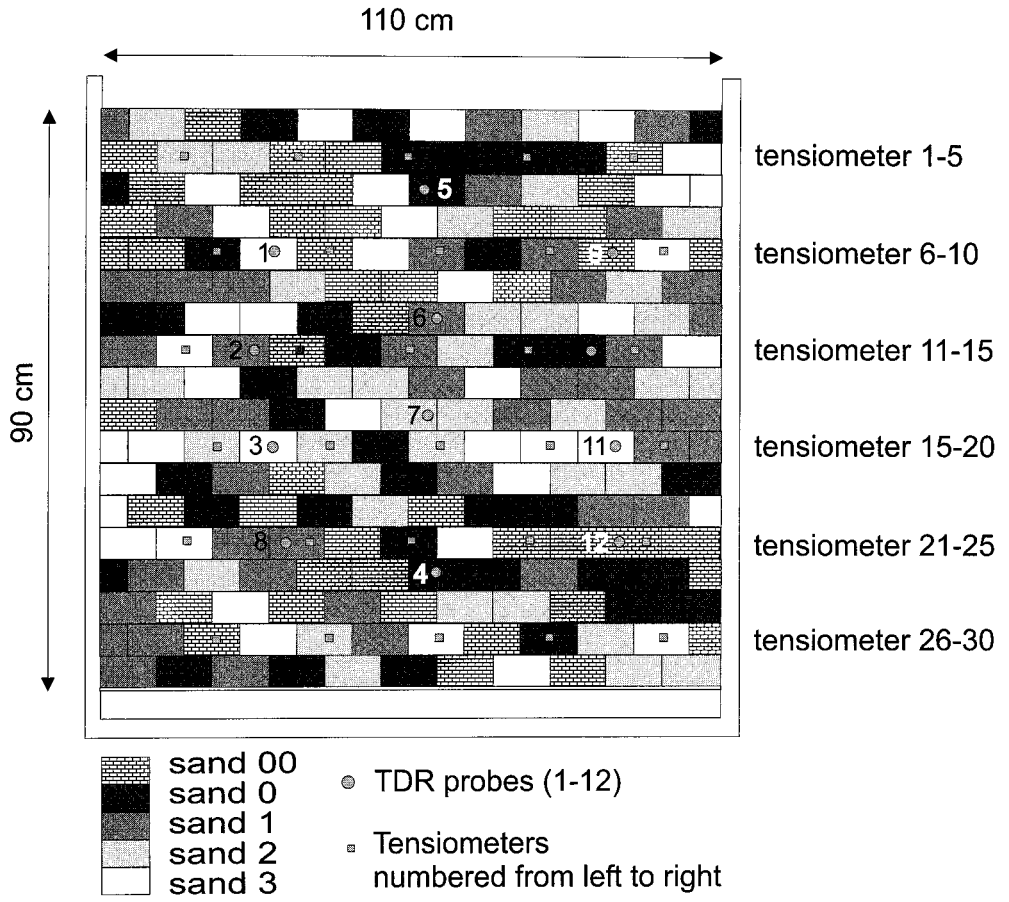

Figure 2. Distribution of homogeneous sands used in tank experiment three and TDR and tensiometer locations.

higher than the desired average in the tank, the suction within the tank dropped to the average level before the location of the first tensiometer 7.5 cm above the bottom plate.

The five homogeneous sands used in the experiments were natural silica sands ranging from coarse (sand 3) to fine (sand 00) sand. Grain size distributions are shown in Figure 3. The unsaturated hydraulic conductivity and water retention curves of the five homogeneous sands were measured prior to the two-dimensional flow experiments. The unsaturated hydraulic conductivity was measured using the long-column method [*Corey*, 1985; *Klute*, 1986]. This method is similar to the method used for the tank experiments, except that a water table is used as the lower boundary condition instead of a porous plate and applied suction. Because of difficulties in controlling the flow rate near saturation, the saturated hydraulic conductivities of the five sands were measured in the long-column setup using a traditional constant-head method. The measured (and parameterized) unsaturated hydraulic conductivity curves are shown in Figure 4. Note that the saturated hydraulic conductivities of the five sands are quite similar, almost within 1 order of magnitude, while the conductivities at higher suctions vary considerably. The retention curves of the homogeneous sands, shown in Figure 5, were measured using the automated syringe pump method as described by *Wildenschild et al*. [1997]. A minimum of three replicate retention curves were determined for each of the five sands, each time using a different sample, but packed to the same porosities as the grid cells in the tank (evidenced by comparing individual and average porosities (θ_s) in Table 1 and 2, respectively). Small variations were observed among the replicates, but the fitted *van Genuchten* [1980] parameters were almost identical for the replicates.

2.2. Tracer Transport

Tracer experiments were carried out in the heterogeneous tank at different steady state flow rates using chloride (Cl^-) and a dye (Eosin B) as tracers. A 250 mL solution containing 10 g/L Eosin B and 25 g/L Cl^- was sprinkled on the soil surface using a syringe. The application took ~1 min, during which the rainmaking device was removed. Solute breakthrough was measured as a flux average at the outlet and at 12 discrete points in the tank using horizontally installed TDR probes. The effluent (outlet) concentration was subject to some degree of mixing in the water reservoir below the porous plate, which had a volume of 1780 mL. Chloride concentrations were measured by ion-selective electrodes, while the dye tracer concentrations were determined by spectrophotometry. The dye tracer was monitored using both video and photographic equipment, enabling qualitative tracking of the transport patterns in the tank. Photographic slides of the tracer movement were scanned and converted to photo CD-ROM images and processed using commercially available software (Corel Photo-Paint from Corel Corporation, Canada).

The TDR probes were not calibrated to provide absolute solute concentrations due to lack of information regarding the maximum (peak) solute concentration passing the individual probes. Instead, they were used to register solute transport

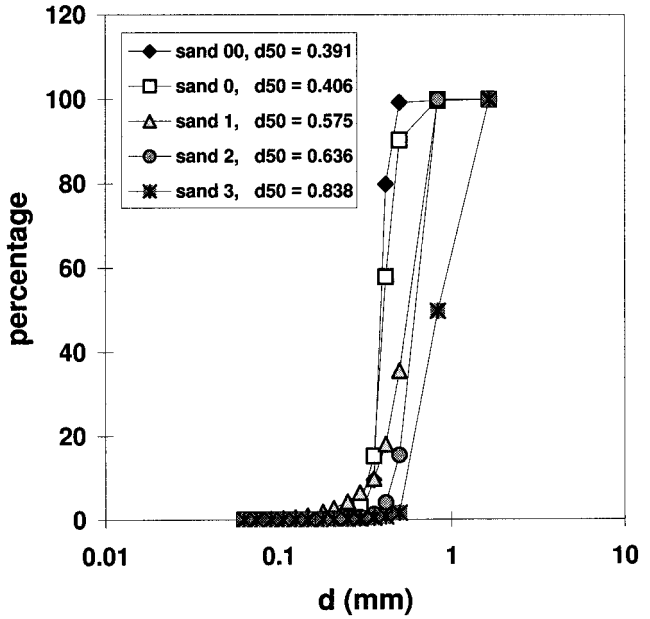

Figure 3. Grain size distributions for the five homogeneous sands.

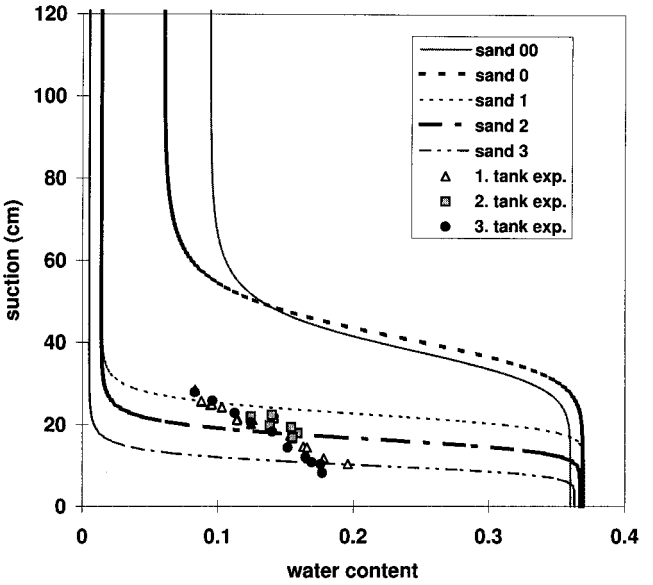

Figure 5. Comparison of the measured retention characteristics of the five homogeneous sands and the three realizations of heterogeneous sand systems.

arrival times and relative breakthrough curves (in addition to water content measurements). Relative breakthrough curves were obtained from the traces scanned by the cable tester (Figure 6). These traces represent the soil electrical resistivity or impedance (y axis) and the electrical pulse travel time through the soil (x axis), the latter depending on the soil water content and the probe length. The signals were digitized, and the resistivities, scanned at the highest travel time values (250) shown in Figure 6, were plotted as a function of measurement time to obtain the relative breakthrough curves. Comparison of the responses of the different probes can be done because the water content is constant in time throughout the experiment and the probes are almost identical in design and manufacture. We also assume that the amplitude of the signal is not seriously affected by the differences in water content of the individual sands and thus justify making qualitative statements as to some probe locations having greater solute concentrations passing by (J. Wraith, personal communication, 1997).

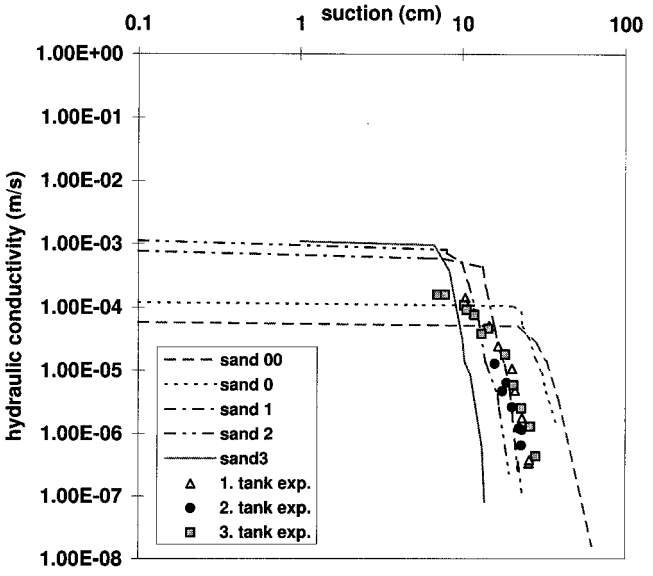

Figure 4. Comparison of the measured unsaturated hydraulic conductivities of the five homogeneous sands and the three realizations of heterogeneous sand systems.

3. Results and Discussion

Two types of quantitative results were obtained from the tank experiments: (1) steady state profiles (corresponding values of suction, water content, and flow rate) from which effective unsaturated hydraulic conductivity and retention curves could be derived and (2) data from transient events that were used for testing of a deterministic two-dimensional model as well as one-dimensional models based on effective hydraulic parameters by *Wildenschild and Jensen* [this issue]. In addition, the solute transport experiments provided qualitative as well as some quantitative information regarding the behavior of water and solutes in heterogeneous systems.

Table 1. Retention and Conductivity Based Parameters for Both Individual Homogeneous Sands and the Heterogeneous Sand System

	Retention-Based				Conductivity-Based	
Sand Type	α	n	θ_s	θ_r	α	n
00	0.026	8.0	0.360	0.094	0.029	5.2
0	0.024	8.3	0.369	0.060	0.034	5.6
1	0.044	12.0	0.370	0.014	0.066	8.4
2	0.060	9.7	0.367	0.014	0.085	6.3
3	0.098	7.8	0.363	0.005	0.110	8.8
Averaged curves (arith.)	0.053	3.0	0.366	0.022	0.050	4.0

Parameters are from *van Genuchten* [1980]. The individual parameters were obtained by fitting van Genuchtens's expression independently to $\theta - \psi$ (pressure cell) and $K - \psi$ (long column) data. θ_s and θ_r are saturated (porosity) and residual water contents.

Table 2. The Number of Grid Cells Occupied by the Individual Sand Types and the Effective Porosities for the Three Realizations

	Number of Grid Cells		
	Realization 1	Realization 2	Realization 3
Sand 00	38	40	46
Sand 0	46	49	39
Sand 1	44	37	45
Sand 2	40	38	37
Sand 3	39	43	40
Average calculated porosity	0.37	0.37	0.37
Average measured porosity	0.39	0.39	0.38

Calculated porosities are derived using weighted averages. Measured average porosity is obtained from the measured amount of each type of sand that was packed into the tank.

3.1. Flow

The effective unsaturated hydraulic conductivity and retention characteristics were measured at consecutive states of steady water flow using the unit mean gradient approach of *Yeh* [1989] and *Yeh and Harvey* [1990]. A uniform, "average" pressure profile was established in the vertical direction by applying suction at the bottom and a constant flux at the top. At steady state conditions the flow is then driven by gravity only, and, consequently, the effective unsaturated hydraulic conductivity corresponds to the applied flux. Consecutive points of the effective hydraulic conductivity-capillary suction curve were obtained by incrementally changing the incoming flux, awaiting steady state, and plotting the measured flux at the outlet against the averaged value of the 30 tensiometer measurements. Analogously, effective retention characteristics were established from simultaneously measured values of suction (30 tensiometers) and water content (12 TDR probes). Both sets of data were subsequently averaged to give one point of the effective retention curve.

The measured retention and conductivity curves for both the individual homogeneous sand types and for the heterogeneous systems were parameterized using the expressions of *van Genuchten* [1980]:

$$S_e = \frac{1}{[1 + (\alpha\psi)^n]^{1-1/n}} \qquad \psi > 0 \tag{1}$$

where S_e is effective saturation, $S_e = (\theta - \theta_r)/(\theta_s - \theta_r)$, θ is the water content, θ_s and θ_r are the water contents at full and residual saturation, respectively, ψ is capillary suction, and α and n are empirical parameters and

$$K = K_s S_e^{\gamma}[1 - (1 - S_e^{1/m})^m]^2 \tag{2}$$

where K_s is the saturated hydraulic conductivity, $m = 1 - 1/n$, and γ is a fitting parameter commonly fixed at 0.5. Values for α and n obtained by independently fitting these expressions to the measured retention (syringe pump method) as well as the measured hydraulic conductivity (long column) data of the five homogeneous sands are shown in Table 1. Also listed in the table are the parametric values for the average retention and hydraulic conductivity curves that are obtained by arithmetically averaging the water contents and the hydraulic conductivities, respectively, of the 5 individual curves at each suction. Directly averaging the parameters would lead to very different parameter sets due to the nonlinear nature of the water retention and hydraulic conductivity curves. Noticeable differences are present between the α and n values obtained using the two sets of data in Table 1, indicating that the parameters obtained from retention curves are not necessarily representative of the unsaturated hydraulic conductivity relationships.

Infiltration experiments were carried out for three different distributions of the five sand types. The number of grid cells occupied by the individual sand types and the average porosities of the three realizations are listed in Table 2. Note that average porosities calculated as weighted averages of the porosities of the individual sands compare well to the values derived from the measured amounts of sand built into each realization. The experiments were designed to ensure that a uniform average pressure profile was present over the entire vertical extent of the tank. The tensiometer readings at the 30 different locations showed some variation in suction between the finer and coarser sand cells. *Yeh and Harvey* [1990] found similar variations in their experiments. An example of the discrete readings and their vertical and total averages and standard deviations is shown in Table 3 for one steady state flow situation. Table 4 shows the statistics of the vertical averages for all steady state experiments of realization number three. Despite some variation in suction among individual cells, averaging the tensiometer readings in either the horizontal or, especially, the vertical direction produced very similar results (Table 3). Thus average suction values for the heterogeneous tank were computed as arithmetic averages of the 30 tensiometers. These averages were assumed to be representative of the equivalent homogeneous system. The same unit mean gradient approach was also used by *Yeh* [1989] and *Yeh and Harvey* [1990].

Figure 7 shows the standard deviations as a function of the average suction of the 30 tensiometers for each steady-state

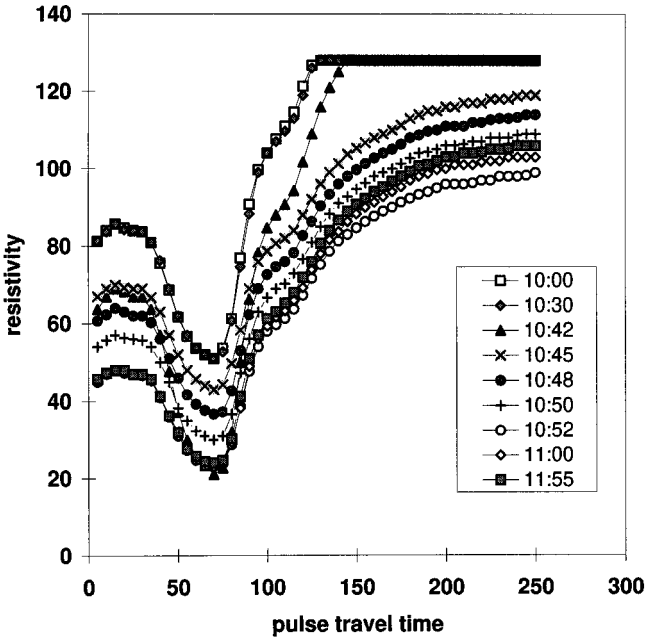

Figure 6. TDR signals (x and y values scanned with the cable tester) as a function of time. Readings at pulse travel times of 250 were used for establishing the relative solute breakthrough curves.

Table 3. Example of 30 Tensiometer Readings at Steady State Flow Conditions With Vertical and Total Averages

	x_1	x_2	x_3	x_4	x_5
z, cm					
82.5	−9.3	−7.9	−9.0	−11.6	−7.7
67.5	−11.6	−9.6	−10.5	−11.9	−8.6
52.5	−5.9	−15.7	−13.7	−11.7	−12.3
37.5	−9.1	−9.7	−7.8	−7.0	−13.9
22.5	−8.2	−13.3	−10.8	−11.9	−9.5
7.5	−13.9	−9.5	−9.2	−9.9	−8.5
Avg.	−9.7	−10.9	−10.2	−10.7	−10.1
s.d.	2.8	2.9	2.0	2.0	2.4
Avg. Overall					
−10.3					
2.4					

	Flow, L/min	Barrier Suction, cm
Avg.	0.57	−11.8
s.d.	0.03	0.8

Flow and barrier suction moments are temporal within the particular steady state step, whereas pressure moments are first temporally then spatially averaged vertically or overall.

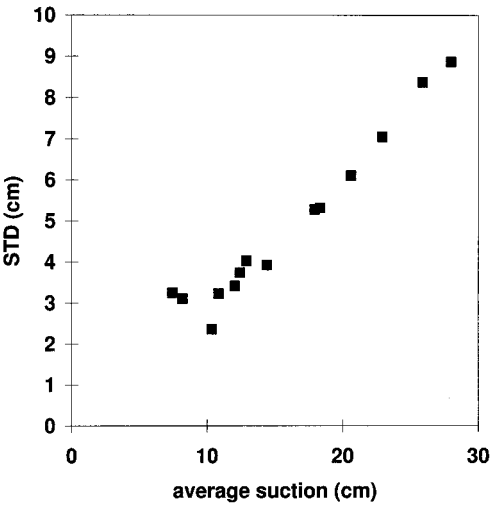

Figure 7. Standard deviation as a function of average suction for the 30 tensiometers used in the tank experiment, realization number 3.

flow situation. There is a notable increase in the standard deviation as the suction increases, a trend that was also reported by *Yeh and Harvey* [1990] and suggested, on the basis of theoretical findings, by *Yeh et al*. [1985a, b, c] and *Mantoglou and Gelhar* [1987a, b, c]. This saturation-dependent standard deviation is not surprising as differences in unsaturated hydraulic conductivity of the five homogeneous sands increase with increasing suction (Figure 4). The variability in hydraulic conductivity causes water to follow increasingly tortuous flow paths with increasing suction (decreasing saturation). This observation also agrees with investigations of the dependence of the hydraulic anisotropy of stratified soils on saturation [*Stephens and Heermann*, 1988; *McCord et al*., 1991a, b]. Even

Table 4. Vertical and Total Averages for All the Steady State Measurements of Tank Experiment Number Three

	Vertical Average of Column of ψ Measurements at Horizontal Position X					Average of 30 Tensiometers	Q, m/s
	x_1	x_2	x_3	x_4	x_5		
Sept. 11 Avg.	−7.1	−8.2	−6.3	−6.7	−10.6	−7.9	1.58E-04
s.d.	1.6	3.2	2.6	2.6	6.4	3.9	
Sept. 12 Avg.	−8.2	−8.9	−7.1	−7.4	−10.9	−8.6	1.58E-04
s.d.	2.1	3.1	2.2	2.0	6.3	3.7	
Sept. 13 Avg.	−9.7	−10.9	−10.2	−10.7	−10.1	−10.3	1.08E-04
s.d.	2.8	2.9	2.0	2.0	2.4	2.4	
Sept. 14 Avg.	−10.2	−11.1	−10.6	−11.9	−10.2	−10.7	9.18E-05
s.d.	4.6	3.5	2.4	3.3	2.5	3.3	
Sept. 15 Avg.	−11.3	−12.0	−11.9	−13.5	−11.4	−11.9	7.61E-05
s.d.	4.8	3.7	2.4	4.0	2.1	3.5	
Sept. 16 Avg.	−14.4	−13.8	−14.2	−15.8	−13.7	−14.5	4.58E-05
s.d.	5.9	3.8	3.2	4.6	1.9	4.0	
Sept. 17 Avg.	−13.9	−12.2	−12.5	−13.6	−12.8	−13.2	3.79E-05
s.d.	6.1	3.6	3.0	4.8	1.9	4.0	
Sept. 18 Avg.	−18.7	−17.4	−18.1	−19.5	−17.7	−18.4	1.78E-05
s.d.	8.5	4.4	4.5	6.2	2.2	5.4	
Sept. 21 Avg.	−17.5	−21.2	−21.5	−22.1	−20.7	−20.7	5.80E-06
s.d.	5.3	7.3	6.6	6.6	5.4	6.0	
Sept. 22 Avg.	−21.0	−23.0	−23.0	−24.6	−23.1	−23.1	2.50E-06
s.d.	9.5	7.7	6.5	7.5	5.4	7.1	
Sept. 26 Avg.	−26.5	−26.0	−24.9	−26.6	−25.3	−26.1	1.28E-06
s.d.	13.3	8.7	7.2	8.2	5.0	8.5	
Sept. 27 Avg.	−27.2	−28.3	−27.4	−29.4	−27.6	−28.2	4.30E-07
s.d.	13.6	9.1	7.7	8.8	6.2	9.0	
Oct. 2 Avg.	−12.6	−12.3	−12.4	−13.6	−11.6	−12.5	4.53E-05
s.d.	6.0	2.8	2.9	4.6	1.9	3.9	
Oct. 3 Avg.	−18.4	−16.9	−18.2	−19.5	−17.2	−18.2	1.62E-05
s.d.	8.4	4.7	4.4	5.4	3.6	5.4	

Vertical average is measured at five different x locations indicated in Figure 1.

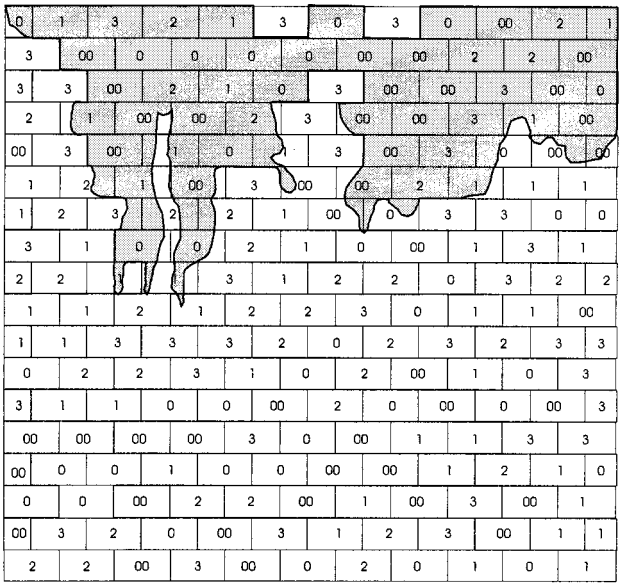

(a)

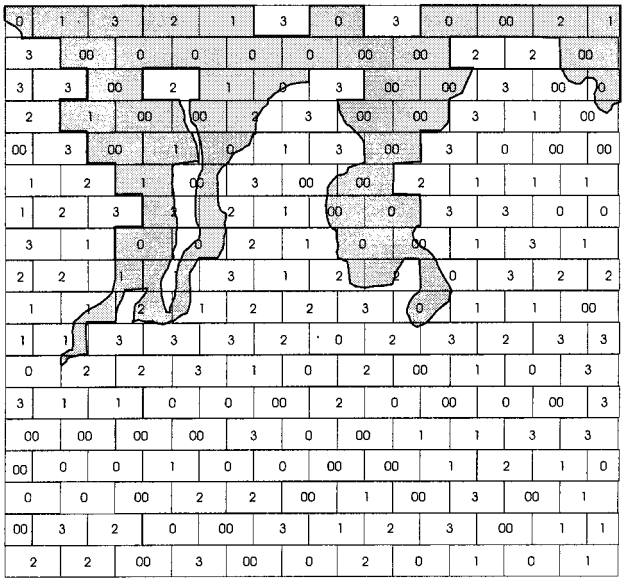

(b)

Figure 8. Solute tracer images corresponding to displacement of 0.05 pore volumes. (a) $q_1 = 4.5\ 10^{-5}$ m/s ($t = 18$ min) and (b) $q_2 = 1.6\ 10^{-5}$ m/s ($t = 48$ min).

though the individual soil types in our heterogeneous setup are isotropic, the results indicate that a large-scale saturation dependent anisotropy may result because of increased lateral flow through high-conductivity zones around the low-conductivity grid cells.

Steady state values of suctions for the three realizations, arithmetically averaged as explained above, are plotted against flow rate measurements to obtain the effective unsaturated hydraulic conductivity relationships in Figure 4 and against arithmetically averaged water contents to obtain the effective retention characteristics in Figure 5. Even though the mean values of the suction varied only within a relatively narrow range, the effective hydraulic conductivity spanned 3 orders of magnitude. Because of difficulties controlling the flow rate close to full saturation, no measurements were made at very small suction heads for the tank experiments. The effective measurements are, in both figures, compared to functions representing the individual homogeneous sands. The plots in Figures 4 and 5 suggest that effective unsaturated hydraulic conductivity and retention functions, if defined as described above, can be identified for our heterogeneous system at least for the investigated flow regime since the measurements form relatively coherent, well-defined curves. Moreover, the unsaturated hydraulic conductivity and retention characteristics for the three realizations having similar statistical properties agree quite well. Even though coherent effective relationships can be derived on the basis of simple averaging of the steady state measurements, this does not necessarily imply that these relationships can be used for prediction of large-scale nonsteady flow processes.

The heterogeneous configuration of the experimental tanks composed of sand blocks having locally very different hydraulic properties promoted far less lateral flow than would be expected for layered sloping systems, including those exhibiting a capillary barrier effect. Because of bypassing of water around the local low-conductivity grid cells, effective conductivities at a particular suction are much higher than the conductivities of the finer sands in the wet range and of the conductivities of the coarser sands at the higher suctions (Figure 4). Observed effective retention functions obtained for the three tank experiments are similarly compared to the individual curves in Figure 5. The measured effective retention values appear to be more influenced by the coarser sands than intuitively expected; that is relatively low water contents are observed at the lower suctions. This trait is more pronounced at low water contents, as the differences in conductivity between the individual sands increase as the water content decreases. Unfortunately, no measurements were obtained in the wet range to confirm this hypothesis. Entrapped air may also be a contributing factor at low suctions.

3.2. Tracer Transport

We will limit discussion of the tracer experiments to results of the third realization, since the best data set was obtained in this experiment. The distribution of sands in this experiment is shown in Figure 2. Two experiments were carried out at steady flow rates of $4.5\ 10^{-5}$ m/s and $1.6\ 10^{-5}$ m/s. Digitized images obtained from photos of the dye tracer are shown in Figures 8a and 8b and Figures 9a and 9b. The flow patterns are clearly very tortuous, with a large part of the tank being completely bypassed by the tracer. In accordance with the shapes of the unsaturated hydraulic conductivity curves of the individual sands, the effect of heterogeneity is much more noticeable at the lower flow rate (higher suction) (Figures 8a and 9b). Dye tracer movement at the lower flow rate was found to be restricted to grid cells having relatively fine material and closely followed the grid cell boundaries because of higher conductivities of these cells at the lower flow rate. At the higher flow rate (Figure 8a and 9a) dye tracer movement was much more uniform with solute spreading more resembling a classic solute displacement front. Similar results were obtained for the tracer experiments in the two other sand configurations.

TDR response curves for the two flow rates of the third realization are shown in Figures 10 and 11. The response curves are plotted on a relative timescale $t' = t/t_{\text{travel}}$ where t_{travel} is travel time from the top of the tank to the position of the TDR probe in question, i.e., distance to the probe divided

by the average measured pore water velocity ($v_{avg} = q_{avg}/\theta_{avg}$). The figures further illustrate the presence of tortuous flow paths caused by differences in the conductivities of the individual grid cells in the heterogeneous tank. Actually, several TDR probes were completely bypassed and did not respond at all. Figures 10 and 11 show that breakthrough (on the t/t_{travel} scale) occur somewhat earlier at the lower flow rate (Figure 11) than at the higher rate (Figure 10) for the three TDR probes (number 4, 8, and 12) located near the bottom of the tank. This finding is in accordance with the dye tracer images (Figures 8b and 9b) and is a consequence of the more tortuous/preferential flow path observed at the lower flow rate (lower saturation). At the lower saturation, flow and transport is confined to a much smaller part of the soil matrix resulting in relatively higher velocities and faster breakthrough. The

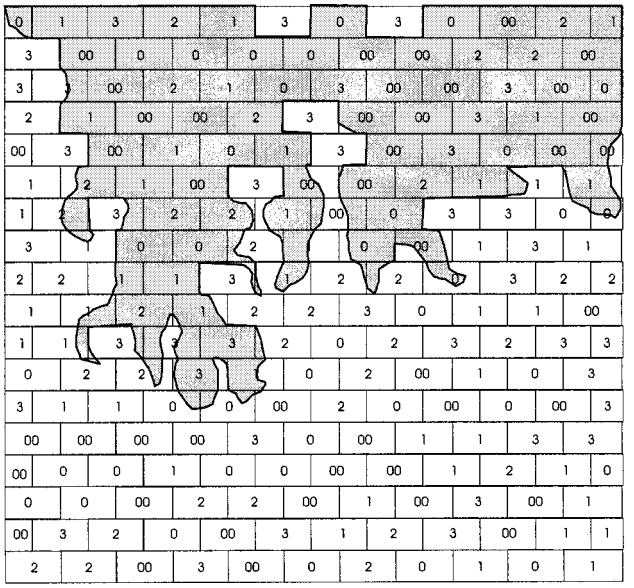

(a)

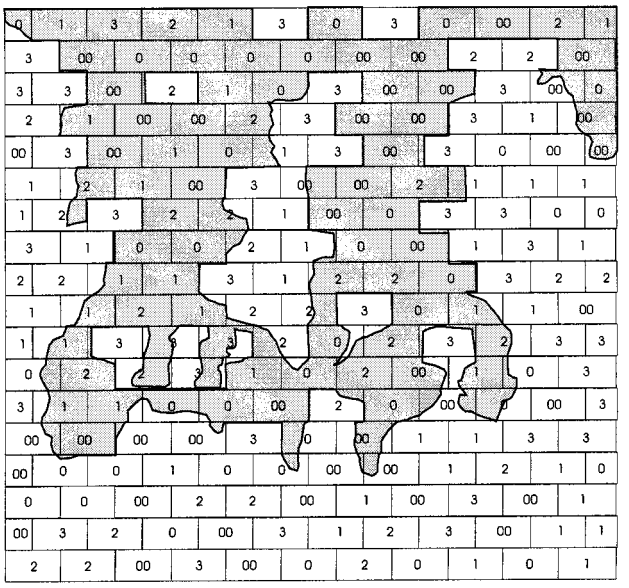

(b)

Figure 9. Solute tracer images corresponding to displacement of 0.08 pore volumes. (a) $q_1 = 4.5\ 10^{-5}$ m/s ($t = 25$ min) and (b) $q_2 = 1.6\ 10^{-5}$ m/s ($t = 72$ min).

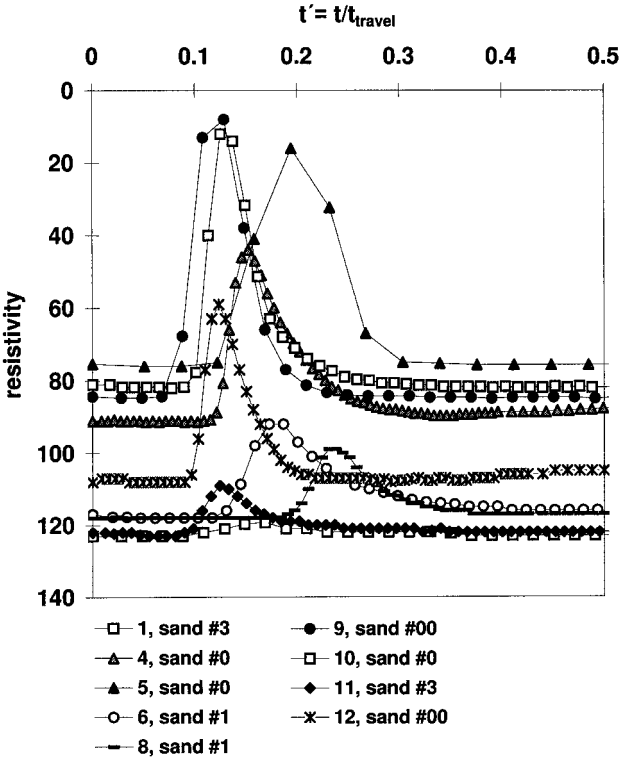

Figure 10. TDR response for solute tracer experiment 3.1 ($q_1 = 4.5\ 10^{-5}$ m/s). Response curves for probes that did not respond to the solute tracer application (i.e., were bypassed) are omitted for clarity.

effect of the differences in saturation/flow rate (the increasingly tortuous/preferential flow path) evidently increases with distance traveled. Accordingly, the breakthrough in probes 9 and 10, located higher in the tank, are comparable for the two different flow rates.

Flux-average breakthrough curves measured at the outlet of the tank at the two different flow rates are shown in Figures 12 and 13 for chloride and Eosin B, respectively. Concentrations are plotted as relative values

$$C' = \frac{C - C_{min}}{C_{max} - C_{min}}$$

based on the background concentration, C_{min}, and the peak concentration, C_{max}, with pore volumes calculated using arithmetic averages of the local water contents. The pore volume scale is used here to allow a comparison of curves measured at different flow rates. The effluent was analyzed for both chloride and Eosin B, since it was uncertain whether the dye tracer would adsorb to the sand. Apparently, this was not the case as both tracers behaved similarly. Displacement of one pore volume took ~5.6 hours and 15.6 hours for the high and low flow rates, respectively. Evidently, flow and transport did not follow the traditional convection-dispersion transport formulation since initial breakthrough occurred already at ~0.1 pore volume. The somewhat earlier breakthrough at the low flow rate, as compared to the higher rate, was also reflected in the TDR traces. The heterogeneity and associated preferential flow process also causes tailing in the effluent. Notice that tailing, as expected, is somewhat more pronounced at the lower flow rate (the curves cross at ~0.35 pore volumes). Fast breakthrough

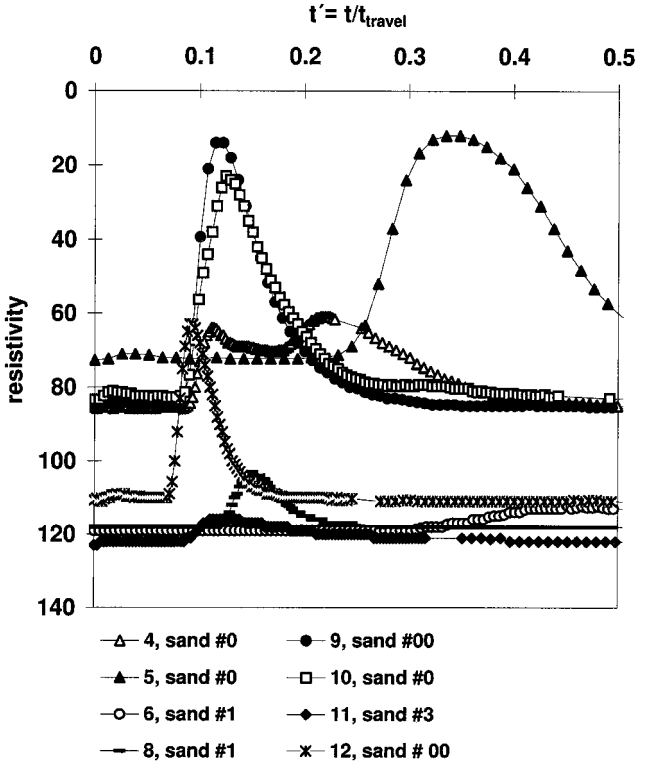

Figure 11. TDR response for solute tracer experiment 3.2 ($q_2 = 1.6\ 10^{-5}$ m/s). Response curves for probes that did not respond to the solute tracer application (i.e., were bypassed) are omitted for clarity.

and tailing are characteristics of preferential flow phenomena and are attributed to flow in areas of relatively high conductivity and to diffusion and entrapment in dead-end or poorly accessible pore space. These flow processes clearly dominate flow and transport for the heterogeneous soil matrix investigated in our study.

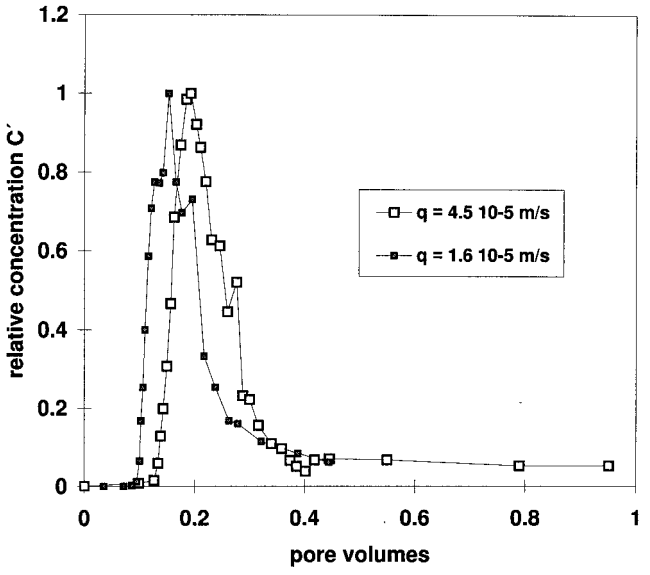

Figure 12. Chloride breakthrough curves for the two experiments.

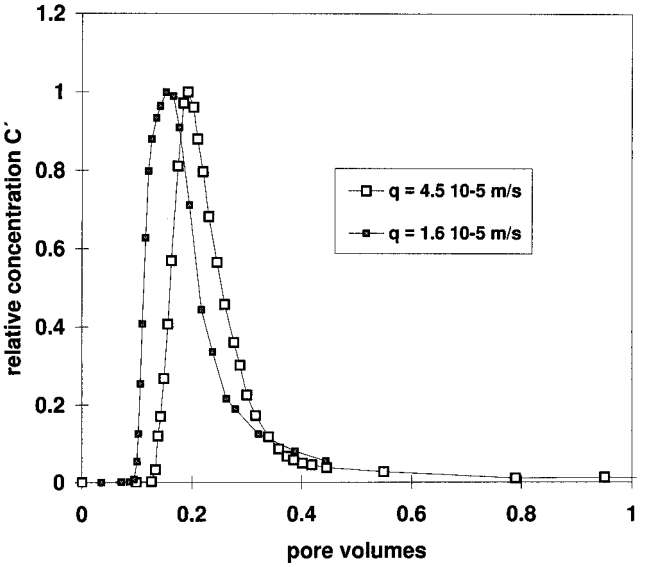

Figure 13. Eosin B breakthrough curves for the two experiments.

4. Conclusions

The concept of effective parameters has been investigated in a two-dimensional tank experiment carried out under controlled laboratory conditions. Effective unsaturated hydraulic characteristics were measured as a function of average suction for three realizations of a random distribution of five homogeneous sands. Effective values were derived from arithmetic averages of the local suction and water content measurements (retention) and, in the case of the unsaturated hydraulic conductivity, from arithmetically averaged measured suctions and the measured average steady state flow rate. Despite a very tortuous flow pattern, similar effective unsaturated hydraulic conductivity and retention curves were obtained for the three realizations. As defined in this study, representative effective unsaturated hydraulic properties seem to exist for the heterogeneous soil configuration and flow conditions investigated. Standard deviations of the average suctions measured in the tank were shown to increase with increasing average suction, indicating a higher degree of heterogeneity of the hydraulic properties at lower saturations. Similarly, solute and dye tracer experiments showed that the tortuosity of flow and transport paths were dependent on the degree of saturation. A more erratic, tortuous transport pattern and earlier breakthrough because of increased preferential flow, was observed at the lower flow rate. The experiments also showed that the effects of the saturation-dependent variability (i.e., increased preferential flow and transport) became more pronounced with the distance traveled, a fact that may have serious implications when large-scale predictions are to be made.

Acknowledgments. M. T. van Genuchten is gratefully acknowledged for his critical review and valuable comments to the manuscript. Thanks also to J. W. Hopmans for his comments and to J. M. Wraith and S. Tyler for help with the interpretation of the TDR signals. M. Butts is acknowledged for input during the initial part of the study. We would like to acknowledge the valuable comments and suggestions we received from reviewer D. B. Stephens and two anonymous reviewers. The Groundwater Research Center at the Technical University of Denmark and the Groundwater Group under the Danish Environmental Program are acknowledged for financial support.

References

Butters, W. L., W. A. Jury, and F. F. Ernst, Field scale transport of bromide in an unsaturated soil, 1, Experimental methodology and results, *Water Resour. Res*., *25*, 1575–1581, 1989.

Corey, A. T., *Mechanics of Immiscible Fluids in Porous Media*, Water Resour. Publ., Fort Collins, Colo., 1985.

Destouni, G., M. Sassner, and K. H. Jensen, Chloride migration in heterogeneous soil, 2, Stochastic modeling, *Water Resour. Res*., *30*, 747–758, 1994.

Hills, R. G., P. J. Wierenga, D. B. Hudson, and M. R. Kirkland, The second Las Cruces experiment: Experimental results and two-dimensional flow predictions, *Water Resour. Res*., *27*, 2707–2718, 1991.

Jensen, K. H., and A. Mantoglou, Application of stochastic unsaturated flow theory, numerical simulations, and comparisons to field observations, *Water Resour. Res*., *28*, 269–284, 1992.

Jensen, K. H., and J. C. Refsgaard, Spatial variability of physical parameters and processes in two field soils, 1, Water flow and solute transport at field scale, *Nord. Hydrol*., *22*, 275–302, 1991a.

Jensen, K. H., and J. C. Refsgaard, Spatial variability of physical parameters and processes in two field soils, 2, Water flow at field scale, *Nord. Hydrol*., *22*, 303–326, 1991b.

Jensen, K. H., and J. C. Refsgaard, Spatial variability of physical parameters and processes in two field soils, 1, Solute transport at field scale, *Nord. Hydrol*., *22*, 327–340, 1991c.

Klute, A. (Ed.), *Methods of Soil Analysis*, *1*, *Physical and Mineralogical Methods*, 2nd. ed., Am. Soc. of Agron. Soil Sci. Soc. of Am., Madison, Wisc., 1986.

Mantoglou, A., A theoretical approach for modeling unsaturated flow in spatially variable soils: Effective flow models in finite domains and nonstationarity, *Water Resour. Res*., *28*, 257–267, 1992.

Mantoglou, A., and L. W. Gelhar, Stochastic modeling of large-scale transient unsaturated flow systems, *Water Resour. Res*., *23*, 37–46, 1987a.

Mantoglou, A., and L. W. Gelhar, Capillary tension head variance, mean soil moisture content and effective specific soil moisture capacity in transient unsaturated flow in stratified soils, *Water Resour. Res*., *23*, 47–56, 1987b.

Mantoglou, A., and L. W. Gelhar, Effective hydraulic conductivities of transient unsaturated flow in stratified soils, *Water Resour. Res*., *23*, 57–67, 1987c.

McCord, J. T., and D. B. Stephens, Lateral moisture movement on sandy hillslope in the apparent absence of an impeding layer, *J. Hydrol. Proc*., *1*, 225–238, 1987.

McCord, J. T., D. B. Stephens, and J. L. Wilson, Toward validating state-dependent macroscopic anisotropy in unsaturated media: Field experiments and modeling considerations, *J. Contam. Hydrol*., *7*, 145–175, 1991a.

McCord, J. T., D. B. Stephens, and J. L. Wilson, Hysteresis and state-dependent macroscopic anisotropy in unsaturated hillslope hydrologic processes, *Water Resour. Res*., *27*, 1501–1518, 1991b.

Mualem, Y., Anisotropy of unsaturated soils, *Soil Sci. Soc. Am. J*., *48*, 505–509, 1984.

Nielsen, D. R., J. W. Biggar, and K. T. Erh, Spatial variability of field measured soil water properties, *Hilgardia*, *42*, 215–259, 1973.

Polmann, D. J., E. G. Vomvoris, D. McLaughlin, E. M. Hammick, and L. W. Gelhar, Application of stochastic methods to the simulation of large-scale unsaturated flow and transport, *Rep. CR-5094*, U. S. Nucl. Regul. Comm., Rockville, Md., 1988.

Polmann, D. J., D. McLaughlin, S. Luis, L. W. Gelhar, and R. Abbabou, Stochastic modeling of large-scale flow in heterogeneous unsaturated soils, *Water Resour. Res*., *27*, 1447–1458, 1991.

Sassner, M., K. H. Jensen, and G. Destouni, Chloride migration heterogeneous soil, 1, Experimental methodology and results, *Water Resour. Res*., *30*, 735–746, 1994.

Stauffer, F., and T. Dracos, Experimental and numerical study of water and solute infiltration in layered porous media, *J. Hydrol*., *84*, 9–34, 1986.

Stephens, D. B., and S. Heermann, Dependence of anisotropy on saturation in a stratified sand, *Water Resour. Res*., *24*, 770–778, 1988.

Topp, G. C., J. L. Davis, and A. P. Annan, Electromagnetic determination of soil water content: Measurements in coaxial transmission lines, *Water Resour. Res*., *16*, 574–582, 1980.

van Genuchten, M. T., A closed-form equation for predicting the hydraulic conductivity of unsaturated soils, *Soil Sci. Soc. Am. J*., *44*, 892–898, 1980.

Wierenga, P. J., L. W. Gelhar, C. S. Simmons, G. W. Gee, and T. J. Nicholson, Validation of stochastic flow and transport models for unsaturated soils: A comprehensive field study, *NUREG/CR-4622*, U. S. Nucl. Regul. Comm., Rockville, Md., 1986.

Wierenga, P. J., R. G. Hills, and D. B. Hudson, The Las Cruces trench site: Characterization, experimental results, and one-dimensional flow predictions, *Water Resour. Res*., *27*, 2695–2705, 1991.

Wildenschild, D., and K. H. Jensen, Numerical modeling of observed effective flow behavior in unsaturated heterogeneous sands, this issue.

Wildenschild, D., K. H. Jensen, K. J. Hollenbeck, T. H. Illangasekare, D. Znidarcic, T. Sonnenborg, and M. B. Butts, A two-stage procedure for determining unsaturated hydraulic characteristics using a syringe pump and outflow observations, *Soil Sci. Soc. Am. J*., *61*, 347–359, 1997.

Yeh, T.-C. J., One-dimensional steady infiltration in heterogeneous soils, *Water Resour. Res*., *25*, 2149–2158, 1989.

Yeh, T.-C. J., and D. J. Harvey, Effective unsaturated hydraulic conductivity of layered sands, *Water Resour. Res*., *26*, 1271–1279, 1990.

Yeh, T.-C. J., L. W. Gelhar, and A. L. Gutjahr, Stochastic analysis of unsaturated flow in heterogeneous soils, 1, Statistically isotropic media, *Water Resour. Res*., *21*, 447–456, 1985a.

Yeh, T.-C. J., L. W. Gelhar, and A. L. Gutjahr, Stochastic analysis of unsaturated flow in heterogeneous soils, 2, Statistically anisotropic media, *Water Resour. Res*., *21*, 457–464, 1985b.

Yeh, T.-C. J., L. W. Gelhar, and A. L. Gutjahr, Stochastic analysis of unsaturated flow in heterogeneous soils, 3, Observations and applications, *Water Resour. Res*., *21*, 465–471, 1985c.

Zaslavsky, D., and G. Sinai, Surface hydrology, 1, Explanation of phenomena, *J. Hydraul. Div. Am. Soc. Civ. Eng*., *107*, 1–16, 1981a.

Zaslavsky, D. and G. Sinai, Surface hydrology. 4. Flow in sloping layered soil, *J. Hydraul. Div. Am. Soc. Civ. Eng*., *107*, 53–64, 1981b.

K. H. Jensen, Department of Hydrodynamics and Water Resources, Technical University of Denmark, 2800 Lyngby, Denmark. (e-mail: khj@isva.dtu.dk)

D. Wildenschild, Department of Earth and Environmental Sciences, Lawrence Livermore National Laboratory, Livermore, CA 94550. (e-mail: wildenschild1@llnl.gov)

(Received June 10, 1997; revised June 5, 1998;
accepted June 8, 1998.)